HELICOPTER ROTOR BLADE VIBRATION CONTROL ON THE BASIS OF ACTIVE/PASSIVE PIEZOELECTRIC DAMPING APPROACH

Sergey Shevtsov
Mechanical Engineering Lab
South Center of Russian Academy
Russia
aeroengdstu@list.ru

Arcady Soloviev
Strength of Materials Dept.
Don State Technical University
Russia
soloviev@math.rsu.ru

Vladimir Acopyan
Physics of Strength Lab
Institute of Mechanics & Applied Mathematics
Russia
akop@math.rsu.ru

Ivan Samochenko
Design Office
Rostvertol Helicopter Production
Russia
rostvertol@aaanet.ru

Abstract

In the presented article a comparative analysis of efficiency of the helicopter rotor blades vibrations suppression by active (controlled) and passive (shunted by electric circuit) piezoelectric patches was performed. For obtaining the information about influence of the external load circuit parameters to behavior of kinematically excited actuator PZT patch the harmonic analysis in the frameworks of 1D electro-elasticity for R, L, C and combined RLC type of a load in a long-wave approximation is performed. For PZT-5H plate working in d31-mode the dependence of oscillations energy harvesting and change of actuator's elastic properties on the patch's geometrical and material parameters were founded. It is shown that for reasonable values of the load capacitance, inductance and resistance the effective suppression of oscillations energy is marked at frequencies greater than 1 kHz only. A flexible structure with surface-bonded PZT patch actuated by PD controller is modelled using Euler-Bernulli beam theory. Emphasis in this study is given to the effect of actuator size and location on the observability, controllability, and stability of the control system. The hybrid vibration damping system with PZT patches actuators was proposed. In this system the vibration suppression on the first flexural modes is yielded with use of the power PD-controllers, and oscillation damping on the torsional and higher flexural modes – by PZT patches loaded on a tuned RC circuits. Efficiency of the offered solution is illustrated by results of the transient analysis of the beam FE model and by experimental data obtained on a scaled model of the helicopter composite rotor blade with bonded flexural and torsional – operated PZT actuators.

Key words

Helicopter rotor blade, Vibration suppression, Piezoelectric patch actuator, Active control, Shunt damping.

1 Introduction

Last two decades considerable amount of research effort has gone into developing a rotorcraft flight vehicle with active control of rotor blades [1-4]. A required component of active rotor blade technology is a sensing/actuation system – the piezoelectric transducers disposed on a controlled flexible host structure. The possibilities to change of rotor blade local bend and twist owing to distributed power actuators action sufficiently enhance a rotorcraft flight conditions, allow to reduce a noise and vibration levels, cruise drag reduction, espesially lift-dependent drag, rotor power consumption, improve of aeromechanical stability, can delay of stall flutter onset for enhancement of flight envelope [4 - 6].

Some engineering solutions of active rotor blade design is using of a high-stroke, on-blade piezostack actuator for a helicopter rotor with trailing-edge flaps where a dual-stage mechanical stroke amplifier also used [2, 5, 7-9]. The macro-fiber composites (MFC), or differently naming, active fiber composites (AFC) [10-12] include a layer of extruded piezoceramic fibers encased in a protective polymer matrix material and the interdigitated electrodes to produce electrical fields in the plane of the actuator. This solution retains the most advantageous features of the early piezocomposite actuators. Hovewer due to technological difficulties of piezoceramic fibers manufacturing the power

piezoelectric actuator formed as plate-like patches or layers bonded to the surface of host structure at this time are most frequently used [6, 13-18]. The correct selection of type, number and location of piezoelectric patche actuators is crucial requirements for efficient control of structural vibration. Therefore, a problem of optimal placement and number of piezoelectric actuators for successful structural control is a very important object. This optimization problem has a further constraint specific for rotary wing aircraft. The above mentioned actuators must be controlled by high voltage transmitted from power amplifiers (so named piezodrivers) through rotated hub, and this is a very complex design task. Due to these circumstances some authors [16-21] offers a passive piezodamping concept that is a low-cost approach and it does not require a complicated electronics. Also the shunt circuit implementation has advantageous [19-25]:

- Passive circuit requiring no external power source.
- Small circuit size.
- Circuit integrity under centrifugal loading.

Passive shunt damping (abbreviated by PSD) always is applied by connecting a passive electrical circuit to the electrode terminals of a piezoceramic patch attached to the host structure. PSD was studied on various structures ranging from experimental beam setups to space truss structures, machining process [14], aircraft applications [6, 26, 29] and occasionally successful results have been obtained. The applications of PSD presented in detail by a review article [27]. An efficiency of PSD applying to suppression of a tools self-excited vibration at relative high frequencies was particularly studied and confirmed by D.J.Inman with coworkers [13, 14, 28], . G.Coppotelli and coworkers [6] developed and experimentally investigated a small unmanned helicopter with flexible rotor blades equiped by the PZT patches working in the PSD mode.

As energy harvesting devices the shunted PZTs convert existing mechanical energy into electrical energy that eventually dissipated into heat. Therefore it is important to understand the features of PZT patch as electric power supply. These problems were considered in [30-35] but par excellence at frequencies closely to resonanses of used PZT patches. In order to reduce the working frequencies for efficient vibration suppression by PSD some authors have used the linear circuit elements such as resistors, capacitors, and inductances [13, 14, 19, 20], the synthetic floating inductors [6, 25], nonlinear diodes [22] etc. A further benefit of PSD is absolute stability in the whole frequency range instead active vibration damping mode where small non-collocation between the sensor and the actuator may cause instability [36-41].

In this paper we discuss the possible application of PSD for vibration suppression of the scaled composite helicopter rotor blade in the operational frequency range. Considering a simplified 1D model of RLC - shunted harmonically excited piezoelectric plate we conclude that "passive" mode can be effectively used for vibration suppression on the high natural modes only. Next we have analytically investigated a flexible structure with active controlled surface-bonded piezoceramic patches using Euler-Bernoulli beam theory. We deduced from here some constraints superimposed on the sensors and actuators size and location for satisfactory damp the desired vibration modes. These results were confirmed by our simulations on the hybrid Comsol/Simulink FEM model and by experimental data obtained on the scaled "active/passive" rotor.

For satisfactory vibration suppression of the flexible rotor blade the combined approach was proposed. According to this approach all active controlled PZT patches must be actuated with low pass filtering preferentially on a first eigenfrequencies. Thus all installed shunted passive PZT transducers will damp high vibration frequencies.

2 The scaled model of active rotor

For manufacturing of (1/6) scaled active rotor (see. fig.1) the composite spars of helicopter tail rotor were used. These spars have length approximately 1.2 meters and close to rectangular D-like cross-section 25*50 mm. For ensure the dynamic similarity of rotated full-sized root hinged helicopter main rotor blade and scaled blade at identical rotation frequencies these scaled blades were equiped by attached tip mass (see Fig.2).

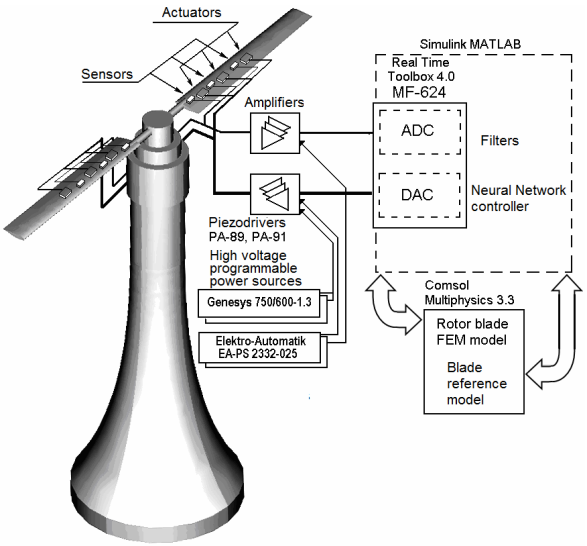

Figure 1. Experimental setup of active rotor's scaled model

The mass and moment inertia of attached tip weights was adjusted for equalize first flapwise and chordwise eigenfrequencies of the scaled and full scale blades.

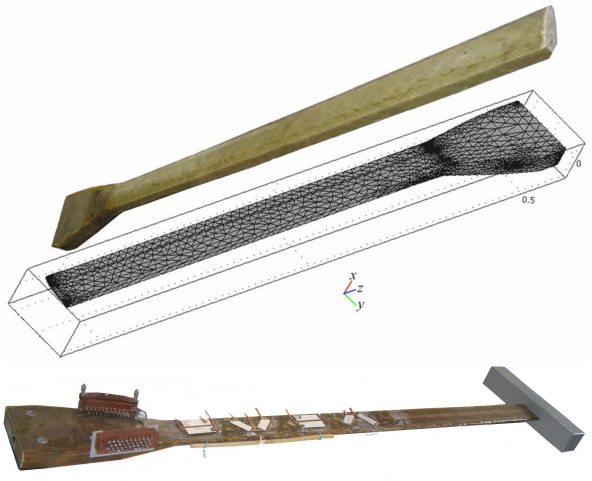

Figure 2. Composite spar for scaled rotor
Top - down:
Originally manufactured, FEM model, equiped by tip mass, and piezoelectric patches

At these conditions two first natural modes of the scaled blade have eigenfrequencies 3 Hz and 8 Hz for the flapwise and chordwise vibration respectively. As rotation frequency decrease up to its operational limit both first vibration frequencies reaches to 10...12 Hz, and second bending vibration frequencies reaches to 20 Hz (flapwise) and 30 Hz (chordwise). This is a frequency range where need the most intensive vibration suppression. At rotation of the helicopter rotor a vibration source caused by dissymmetry of lift acting on the advancing and retreating blades. In the scaled model flapwise and chordwise vibrations were forced by two electromagnets installed on the way of the blades tips. At each appointments of blade tip with these electromagnets rotor blades undergoes a transversal shock and vibrated preferentially on the low natural frequencies.

3 Harmonically excited PZT patch's 1D model

In above mentioned article [6, 13, 14, 19-24] where passive piezoelectric vibration damping was investigated an operational frequency range locates over 1 kHz. At harmonic analysis of UAV's slender rotor blade with attached PZT patches loaded on RL circuits the authors [6] communicates well achieved vibration reduction data at 58 Hz. Here we try to perform a quantitative estimate of passive PSD efficiency for available rotor blade vibration suppression at frequencies around 10...50 Hz. First we study an amplitude-frequency response of a simplest PZT patch 1D model with combined RLC load.

Now consider a thin PZT plate reached along x-axis polarized in z-direction (perpendicular to the major side) and subjected to the harmonical cinematic excitation along longest side as shown on the fig.3.

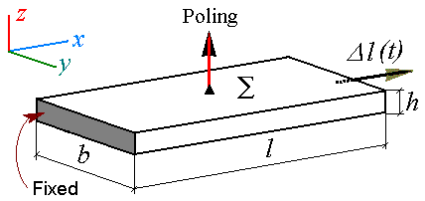

Figure 3. Schematic view of the modeled PZT patch

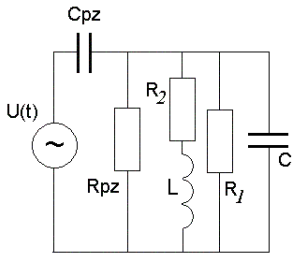

Figure 4. Generalized scheme of PZT patch connected to arbitrary linear electric load

Upper and lower surfaces of PZT plate are covered by conducted layer, and its electrical load can have an arbitrary type (fig. 4). Thus our piezoelectric plate works as strain sensor in $e_{31}(d_{31})$ mode.

Constitutive equations of piezoelectricity in stress-charge form are

$$\begin{cases} \boldsymbol{\sigma} = \mathbf{c}^{E} \cdot \mathbf{S} - \mathbf{e}^{\mathbf{T}} \cdot \mathbf{E} \\ \mathbf{D} = \mathbf{e} \cdot \mathbf{S} + \boldsymbol{\varepsilon}_{\mathbf{S}} \cdot \mathbf{E} \end{cases} \tag{1}$$

where $\boldsymbol{\sigma}$,$\mathbf{S}$ - stress and strain tensors respectively - in matrix notation both 6×1 vectors, $\mathbf{D}$,$\mathbf{E}$ - electric displacement (charge density) and electric field respectively - 3×1 vectors, $\mathbf{c}_{\mathbf{E}}$ - stiffness 6×6 matrix at constant (zero) electric field, $\mathbf{e}$ and transposed $\mathbf{e}^{\mathbf{T}}$ - piezoelectric coupling coefficients for stress-charge form - 3×6 and 6×3 matrices respectively, $\boldsymbol{\varepsilon}_{\mathbf{S}}$ - electric permittivity at constant (or zero) strain - diagonal 3×3 matrix. For simplicity we assume that our plate is piezoelectric 1D leg oriented along x-axis and we neglect all transversal effects. Then equation system (1) was simplified to

$$\begin{cases} \sigma_x = c_{11}^{E} \cdot S_x - e_{31} \cdot E_z \\ D_z = e_{31} \cdot S_x + \varepsilon_{33}^{S} \cdot E_z \end{cases}. \tag{2}$$

Let down surface of the piezoelectric plate is grounded and upper plane that have a surface area $\Sigma = l \cdot b$ was supported under potential V permanent along the plane. Let also the right tip elongation vary harmonically according to the law

$$\Delta l(t) = \delta \cdot \exp(i\omega t). \tag{3}$$

Then long wave approximation lead to such equations

$$\begin{cases} \sigma_x = c_{11}^E \cdot \exp(i\omega t) \cdot \delta / l - e_{31} \cdot E_z \\ D_z = e_{31} \cdot \exp(i\omega t) \cdot \delta / l + \varepsilon_{33}^S \cdot E_z \end{cases}. \quad (4)$$

This admission is true in a frequency range less than first natural frequency of PZT patch. For considered plate its first eigenfrequency (bending in the plane of min stiffness is about 1 kHz). However, when the plate is bonded on the surface of host structure all eigenfrequencies of the composed structure (host plus PZT plate) will be determined by large host structure not by small PZT plate. And operational frequency range for the host structure vibration damping locates from ones Hz to 150...200 Hz. Therefore our admission is well founded.

Denote the amplitude values of E_z as E_0, and for σ_x as σ_0. If PZT plate is loaded on some electric circuit with impedance Z then passed electric current in the complex form can be presented as

$$\begin{aligned} & i_z = \dot{D}_z \cdot \Sigma \Rightarrow \\ & i\omega \cdot e^{i\omega t} \left[e_{31} \cdot \delta / l + \varepsilon_{33}^S \cdot E_0 \right] \Sigma = -\frac{E_0 \cdot h}{Z} e^{i\omega t} \end{aligned} \quad (5)$$

We obtain from here the amplitude of electric field

$$E_0 = -\frac{i\omega e_{31} \delta / l}{h/(\Sigma Z) + i\omega \varepsilon_{33}^S}, \quad (6)$$

and voltage in the complex form

$$V = \frac{i\omega e_{31} \delta h / l}{h/(\Sigma Z_L) + i\omega \varepsilon_{33}^S} = \frac{i\omega e_{31} \delta b}{Y_L + Y_{Cpz}}, \quad (7)$$

where Y_L, Y_{Cpz} - electrical conductance of the load and PZT plate (capacitive) respectively. Considering dimensions of the piezoelectric (PZT-5H) plate l=5 cm, h=1 mm, b=1.5 cm one can be obtain the capacity of PZT plate $C_{pz} \approx 0.01 \mu F$. Calculation of eqs.7 show that for amplitude of patch tip displacement δ=0.02 mm and arbitrary load resistances at increasing of the excitation frequency the real part of voltage yearns to the common limit $V_{\lim} = -e_{31} \delta b / C_{pz} \approx 230V$.

For arbitrary load conductance Y_L an equivalente conductance will be $Y = Y_1 + iY_2$, where $Y_1 = \mathrm{Re}(Y_L + Y_{Cpz})$, $Y_2 = \mathrm{Im}(Y_L + Y_{Cpz})$; then output voltage and electric current are

$$V = \frac{i\omega e_{31} \delta b}{Y_1 + iY_2}, \; I = \frac{i\omega e_{31} \delta b}{Y_1 + iY_2} Y_L. \quad (8)$$

Real part of electric power (equal to mechanical loss)

$$\mathrm{Re}(W) = \mathrm{Re}\left(h\Sigma \cdot \int_0^{2\pi/\omega} \sigma \cdot \frac{d\bar{\varepsilon}}{dt} dt \right) = \frac{Y_1}{2} \frac{(\omega e_{31} \delta b)^2}{Y_1^2 + Y_2^2}, \quad (9)$$

and mechanical stress in the PZT plate

$$\sigma_x = \frac{\delta}{l} \cdot \left\{ \left[c_{11}^E + \frac{e_{31}^2 \cdot \omega C_{pz} Y_2}{\varepsilon_{33}^S \left(Y_1^2 + Y_2^2 \right)} \right] + i \frac{e_{31}^2 \cdot \omega C_{pz} Y_1}{\varepsilon_{33}^S \left(Y_1^2 + Y_2^2 \right)} \right\} \quad (10)$$

In last expression first summand is an efficient elastic modulus and second one is a damping factor. The calculation results for eqs. (9) and (10) at different inductance, R_l=100 kOhm and C=1 F are presented on a fig. 5.

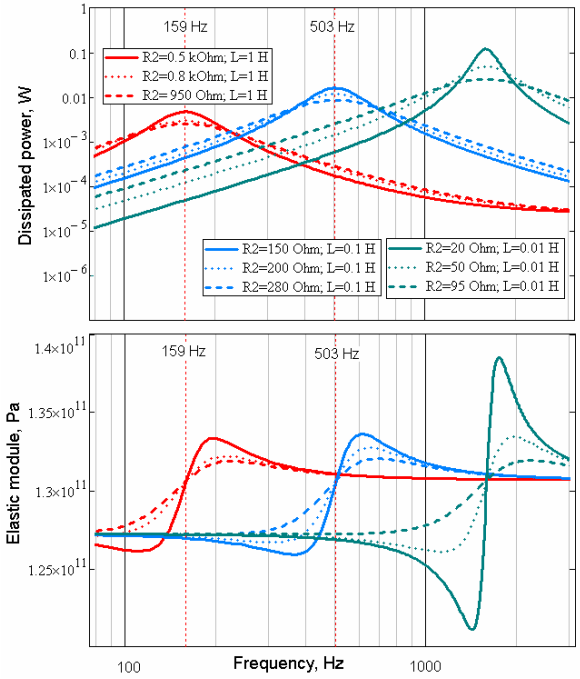

Figure 5. Electric power dissipated on an electric load (above) and efficient elastic modulus vs excitation frequency (explanation in text)

One can see that decreasing of the shunt resistance lead to expansion and to erosion of the power resonance peaks. Besides decreasing of the serial resistance R_2 (together with corresponding diminishing of inductance lead to peak shift in area of lower frequencies and increase the power maximum. It is simple to deduce that at frequency ω growing to infinity the additive factor in expression of efficient elastic module yearns to its limit value $e_{31}^2 / \varepsilon_{33}^S$ that not depends on the load's impedance. The variation of the effective module is not monotonic and has a peak at frequency rather greater than power's peak. Calculations (8) - (10) at different values of load inductance and capacitance show that PSD in a low frequency range is not efficient for

vibration damping as well as stiffening of the host structure. The sizeable increasing of inductance not changes these conclusions considerably. Therefore even using of special electric circuit for a synthetic inductor in order to avoid an unacceptable weight of natural inductance is not a good solution for suppresses by harvesting a low frequency vibration.

4 Smart beam with two opposite placed PZT patches. Transient and modal analysis

For investigation of active/passive composite beam vibration suppression the FEM models presented on a fig. 6 is used. It consists of two PZT patches placed along a beam axis. These actuator patches were attached to the upper and lower surfaces of a composite spar. Bonded surfaces of transducers were grounded, and theirs poling vectors are oriented identical. All numerical experiments were performed on a simplified cantilever composite beam with rectangular cross-section by means of finite element package Comsol Multiphysics in the Structural Mechanics - Piezoelectric mode. This mode includes full system equation of anisotropic electro-elasticity, where coupled behavior of electrical and mechanical subsystem was considered.

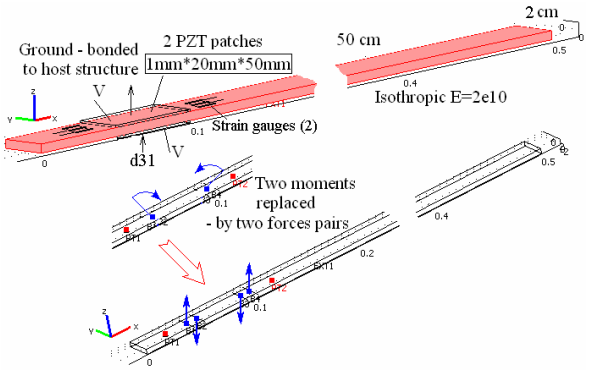

Figure 6. FE model of investigated smart beam

At simulation of passive piezoelectric shunt damping the electric potentials V_1, V_2 generated by patches were determined from equations, solved on each integration step

$$V_i = R_i \int_{\Sigma} (\mathbf{J} \cdot d\mathbf{s}); i = 1,2, \qquad (11)$$

where R_i - shunt resistance, and integrals express the currents through shunts were evaluated from electric current density $\mathbf{J}$ normal to patch surface $d\mathbf{s}$.

At simulation of active piezoelectric damping the electric potentials V_1, V_2 supplied to patches were calculated from feedback equation

$$V_i = k_s \varepsilon_x + k_v \dot{\varepsilon}_x; i = 1,2, \qquad (12)$$

where strains $\varepsilon_x = 0.5\left(\varepsilon_x^1 + \varepsilon_x^2\right)$ and its velocities $\dot{\varepsilon}_x = 0.5\left(\dot{\varepsilon}_x^1 + \dot{\varepsilon}_x^2\right)$ were averaged by integration in environ of points P_1, P_2 on the surface of beam close to piezoelectric patches. In order to increase an intensity of vibration damping at low excitation frequencies we have investigated active vibration mode with feedback (see eq. 12) at different values of parameters k_s, k_v. The first parameter modifies an equivalent dynamical stiffness of host structure whereas second one has influence on a structural damping. Moreover, both parameters depend on vibration frequency. It is established in our numerical experiments that global structural damping of investigated beam is less sensitive to k_s variation. It may be explained by small dimensions of patches relative to host beam, and also by results argued in the part 2. However, a feedback gain k_v renders essential influence to the damping process, increasing an apparent local dissipation of the beam. Unfortunately, against a case of passive damping the active mode is characterized by low stability and can be inclined to self-excitation. The passive scheme is deprived of this deficiency at all. In order to clear up an origin of mentioned instability we have considered the smart beam excited by tip force.

It is known that action of PZT patch on the beam equivalent to two bending moments [13, 16, 38]. Replacing these two PZT acting moments by two pairs of forces we obtain such Euler-Bernoulli beam equation

$$YJ\frac{\partial^4 w(x,t)}{\partial x^4} + c_a\frac{\partial w(x,t)}{\partial t} + \rho S\frac{\partial^2 w(x,t)}{\partial t^2} + \theta V(t)\left\{\begin{matrix}\delta(x-x_1+\varepsilon)-\delta(x-x_1-\varepsilon)-\\ \delta(x-x_2+\varepsilon)+\delta(x-x_2-\varepsilon)\end{matrix}\right\} = F(t)\delta(x-x_b) \qquad (13)$$

where ε is the half-distance between forces of pair, θ - electro-mechanical coupling term, and feedback potential is proportional to bending strain and its velocities in the measuring points x_3, x_4

$$V(t) = k_s\left[w''(x_3,t) + w''(x_4,t)\right] + k_v\left[\frac{\partial w''(x_3,t)}{\partial t} + \frac{\partial w''(x_4,t)}{\partial t}\right]. \qquad (14)$$

Applying the known separation technique

$$w(x,t) = \sum_j T_j(t)\cdot\phi_j(x), \qquad (15)$$

where $\phi_j(x)$ is eigenfunction and $T_j(t)$ is the modal response of the j-th mode, after multiplication on $\phi_n(x)$ and performing of integration spread over beam length [0;*l*], using the orthogonality conditions

$$\int_0^l \phi_j(x)\phi_n(x)dx = \delta_{jn} \qquad (16)$$

we obtain the infinite equation system for modal responses

$$\ddot{T}_n + \frac{c_a}{\rho S}\frac{\partial w(x,t)}{\partial t}\dot{T}_n + \frac{YJ}{\rho S}\left(\frac{\lambda_n}{l}\right)^4 T_n + \frac{\theta V(t)}{\rho S}\left\{\begin{matrix}\phi_n(x_1-\varepsilon)-\phi_n(x_1+\varepsilon)-\\ \phi_n(x_2-\varepsilon)+\phi_n(x_2+\varepsilon)\end{matrix}\right\} = F(t)\phi_n(x_b) \qquad (17)$$

Then feedback potential will be

$$V(t) = \sum_j \left(k_s T_j + k_v \dot{T}_j\right)\cdot\left[\phi_j''(x_3)+\phi_j''(x_3)\right]. \qquad (18)$$

In the last two equations there are factors determining the observability of the beam dynamic state

$$\left[\phi_j''(x_3)+\phi_j''(x_3)\right]$$

and its controllability

$$\left\{\phi_n(x_1-\varepsilon)-\phi_n(x_1+\varepsilon)-\phi_n(x_2-\varepsilon)+\phi_n(x_2+\varepsilon)\right\}.$$

Really, if sign of the beam curvature changed on the observation points x_3, x_4 the multiplier $\left[\phi_j''(x_3)+\phi_j''(x_3)\right]$ can be undefined. Thus, damped natural mode cannot change its sign between observation points, and distance between observation points must be less then half of damped mode shape.

Beside, the term

$$\left\{\phi_n(x_1-\varepsilon)-\phi_n(x_1+\varepsilon)-\phi_n(x_2-\varepsilon)+\phi_n(x_2+\varepsilon)\right\}$$

can be considered as second order finite difference of n-th eigenfunction. Therefore for successful suppression of n-th vibration mode sign of this term must be constant along the PZT patch. Obtained conclusion superimposes the strong constraint on the longitudinal dimension of PZT patch that also must be less then half of damped mode shape.

Unfortunately, satisfactions of mentioned constraints not guarantee the successful controllability of vibration damping process. As right part of active damping eq. (17) consist the infinite series (18) of values depended on all natural modes, some modes can be reinforced.

These circumstances can be illustrated through example of the beam free vibration damping. For initial conditions we assume a beam axis is immovable and deformed according to 2nd natural mode shape. In the series determining the feedback potential we retain first three members only: for 1st, 2nd, and 3rd mode. The structure of obtained system equation shows that at presence of feedback the different vibration modes can interact. Really, on the first time chart (see fig.7) one can see the natural damping process caused by air viscosity only. Vibration on the 2nd eigenfrequency is fully harmonical, and 1st and 3rd modes are not excited.

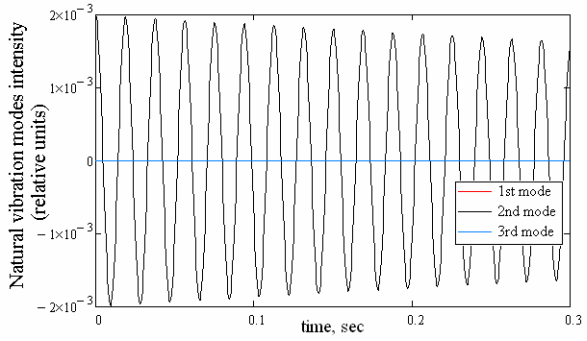

Figure 7. Time chart of the beam natural vibration modes (at absence of feedback)

At feedback switching on we observe an intensive damping of the 2nd mode, but originating of vibration on the 1st and 3 modes (see fig. 7).

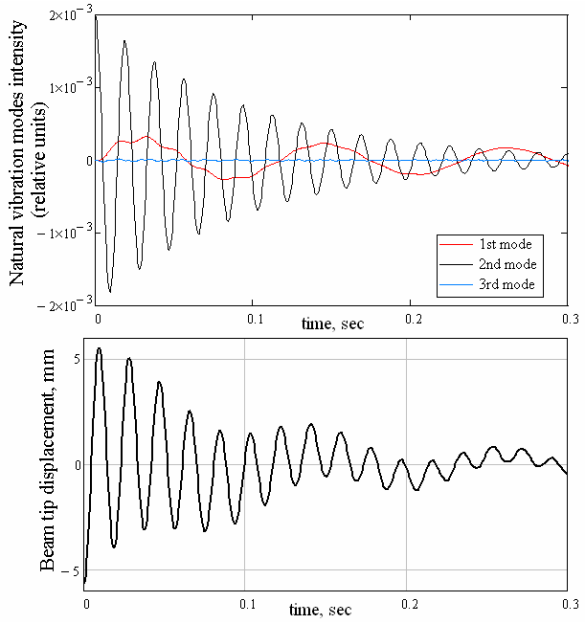

Figure 8. Time chart of the beam natural vibration modes (above) and beam tip displacement (below) (intermediate feedback gain)

A further growth of the feedback gain lead to the oscillations on the 1st mode with amplitude comparable damped vibration amplitude. Lastly we can observe the self excitation on the 3rd natural mode.

In order to avoid these undesirable phenomena one can propose the strong selection of the PZT patches dimensions, location, and (or) filtering of the measured signal in the needed frequency band. Obvioiusly any another artificial means (including artificial neural networks, etc.) cannot retrieve this situation.

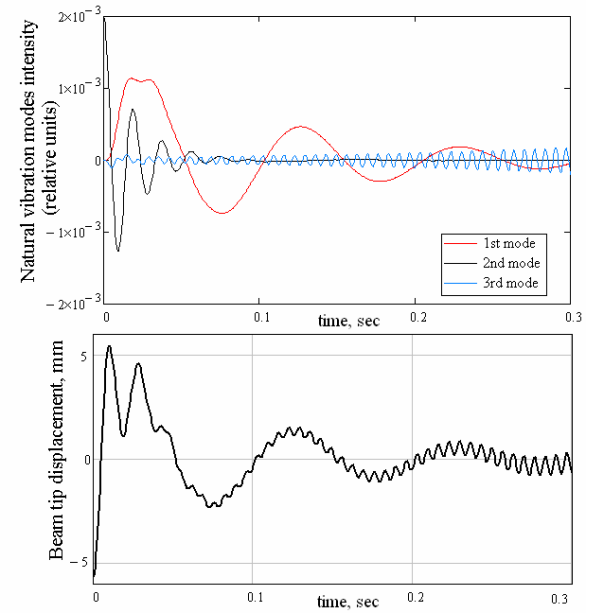

Figure 9. Time chart of the beam natural vibration modes (above) and beam tip displacement (below) (incremented feedback gain)

5 Smart rotor blade. Experimental results

In the presented work we try to perform a quantitative estimate of the combined active and passive piezoelectric patch vibration damping for available rotor blade vibration suppression at harmonical and impulse tip loads. All electric signals from tensometers strain gauges were digitized by multichannel MF624 Humusoft ADC/DAC adapter working under Real Time Toolbox soft module implemented as submodule of Simulink MATLAB soft package. Therefore all signals handling operations were supported by Simulink's program equipment (including filters, phase delay, amplifiers, spectrum analyzers, scopes etc.) functioning in real time (accelerated) mode. All control signals were formed by such scheme also.

Our experiments have shown that active vibration damping is more efficient for harmonical excitation whereas passive mode can be successfully used for suppress the large spectrum oscillations caused by impulse load. At working of active suppression system usually a low frequency vibration beats appear. This case is presented on a fig.10, where the time charts of a bending strain (yellow curves) and normalized feedback voltage (magenta) at harmonical excitation on the 2nd flexural mode are shown. The beat vibrations with low frequency originated after feedback switch on (above) can be suppressed by decreasing of the k_v feedback gain and bandpass digital filtering (below).

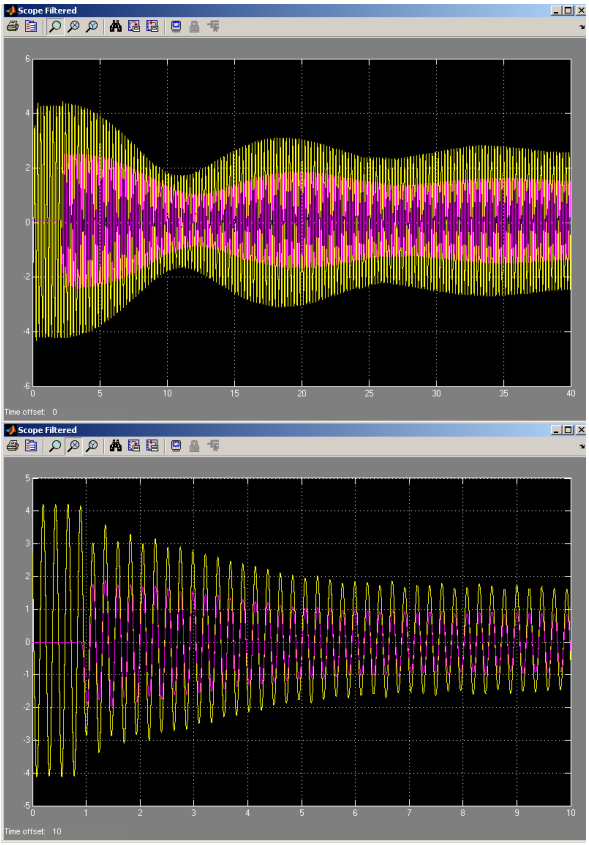

Figure 10. Time charts of harmonically excited beam vibrations damped by active PZT patch control (explanation in text)

The case of PSD of "Hammer excited" vibration of such blade is shown on a fig.11, where upper chart present undamped vibrations (electric potential from open-ended transducer), and lower chart - damping by using two opposite placed piezoelectric patches shunted on the 500 kOhm resistance.

These experimental results confirm theoretical outlets. And on the basis of obtained results the combined vibration suppression method including concurrent using of active controlled and passive (shunted by electric circuit) PZT patches is proposed.

6 Conclusion

The functional features of the power active and passive PZT patch actuators for the beam vibration suppression are investigated.

Frequency responce functions of mechanical stiffness and energy dissipation of RLC - shunted small PZT patch were obtained on a simplified 1-D model. These dependences show the unsatisfactory effectiveness of PSD patches for change the dynamic properties (natural modes and eigenfrequencies) and structural damping of the host structure, especially at low frequencies range.

It is established by finite element transient analysis of beam structure with bonded PZT patches controlled by feedback that formed as linear function of local strain and strain velocity of the structure that such active working mode can be stable at relatively small feedback, and in the narrow frequency band. Moreover, due to nonlinearity of a coupled electro-mechanical distributed control system the suppressed high frequency vibration can be transformed to the vibration on the other forms.

For satisfactory PZT -based vibration suppression the combined approach was proposed. According to this approach all active controlled PZT patches must be actuated with narrow frequency band, filtering preferentially on a first eigenfrequencies. Thus all installed shunted passive PZT transducers will damp high vibration frequencies on the flexural and torsional modes.

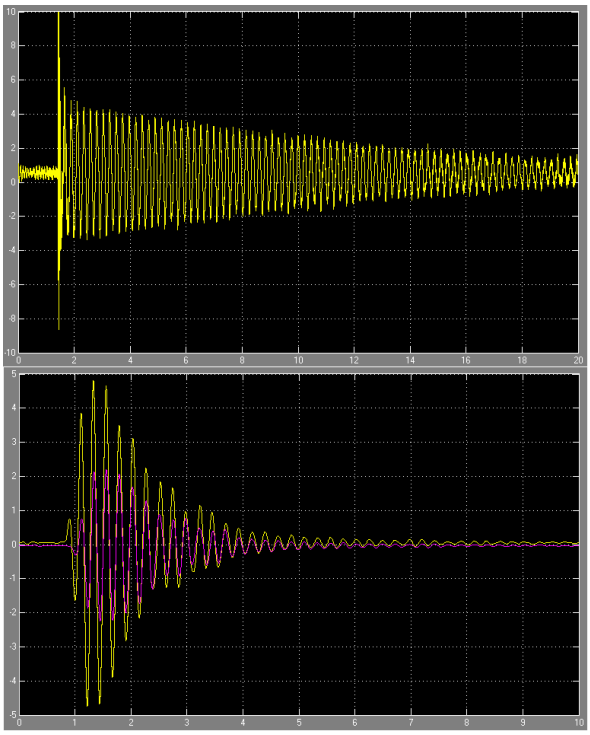

Figure 11. Time charts of the beam vibrations caused by impact load on a beam tip (above) and PSD results (results)

References

1. Sater, J.M., Lesieutre, G., Martin, C. (2006) A smarter transition for smart technologies. *Aerospace America*. June 2006, pp.18-21
2. Maucher, C.K., Grohmann, B., and Janker, P. (2005) Review of Adaptive Helicopter Rotor Blade Actuation Concepts, *Proc. 9th Adaptronic Congress*. Gottingen, 31 May – 1 June 2005, p.12
3. Cooper, J.E. (2007) Adaptive Aeroelastic Structures. In *Adaptive Structures. Engineering Applications*. Eds. D.Wagg and oth., J. Wiley & Sons. pp.137-162
4. Grohmann, B. (2007) Actuators and Systems for Morphing A/C. *Actuation & Smart Structures Conf.* Nov. 5-7, Munich, p.18
5. Janker, P., and oth. (2008) New Actuators for Aircraft and Space Applications. *Proc. on the 11th Int. Conf. on New Actuators*. Bremen, Germany, June, 9 – 11, pp. 346-354
6. Coppotelli, G., Agneni, A., and Balis Crema, L. (2008) Vibration Reduction of a Rotorcraft UAV Using PZT Patches. *Proc. of ISMA 2008 conf*. Leuven, Belgium. Sept. 16-19, pp. 157-168
7. Grohmann, B., Maucher, C.K., and Janker, P. (2008) Embedded Piezoceramic Actuators for Smart Helicopter Rotor Blades. *Proc. of 49th AIAA/ASME/ASCE/AHS/ASC Structures, Structural Dynamics, and Materials Conf., 7 – 10 April 2008*, Shaumburg, Il, p.10
8. Zhang, J., Smith, E.C., and Wang, K.W. (2004) Active-Passive Hybrid Optimization of Rotor Blades with Trailing Edge Flaps. *J. of the American Helicopter Society*, **V. 49**, **No. 1**, pp. 54–65.
9. Lee, T., Chopra, I. (2000) Design Issues of a High-Stroke, On-Blade Piezostack Actuator for a Helicopter Rotor with Trailing-Edge Flaps. *J. of Intelligent Material Systems and Structures*, No.11, pp.328-342
10. Bent, A.A., Hagood, N.W., and Rodgers, J.P. (1995) Anisotropic Actuation with Piezoelectric Fiber Composites. J. of Intelligent Material Systems and Structures, No.6, pp.338-350
11. Rodgers, J.P., Hagood, N.W., and Weems, D.B. (1997) Design and Manufacture of an Integral Twist-actuated Rotor Blade. *Proc. of 38th AIAA/ASME/AHS Adaptive Structures Forum*, Kissimmee, FL, pp.18
12. Bilgen, O., and oth. (2007) Morphing Wing Micro-Air-Vehicles via Macro-Fiber- Composite Actuators. *Proc. of 49th AIAA /ASME /ASCE /AHS /ASC Structures, Structural Dynamics, and Materials Conf.*, 23 – 26 April 2007, Honolulu, Hawaii, p.16
13. Erturk, A., and Inman, D.J. (2008) Analytical Modeling of Cantilevered Piezoelectric Energy Harvesters for Transverse and Longitudinal Base Motions. *Proc. on the 49th AIAA/ASME /ASCE/AHS/ASC Conf*. Schaumburg, IL. p.36
14. Erturk, A., and Inman, D.J. (2008) Piezoelectric shunt damping for chatter suppression in machining processes. *Proc. of ISMA 2008 conf*. Leuven, Belgium. Sept. 16-19, pp. 193-208
15. Maxwell, N.D., Asokanthan, S.F. (2004) Modal characteristics of a flexible beamwith multiple distributed actuators. *J. of Sound and Vibration*. **V. 269**, pp.19-31

16. Zhou, S., Liang, C., and Rogers, C.A. (1995) Integration and Design of Piezoelectric Patch Actuators. *J. of Intelligent Material Systems and Structures*,**V.6**, pp.125-133
17. Shevtsov, S., Soloviev, A.N., Bragin, S. (2008) Structural Optimization of Distributed Actuation System for Improve an Efficiency of Smart Composite Spar Vibration Damping. *Proc. of ISMA 2008 conf.* Leuven, Belgium. Sept. 16-19, pp. 339-352
18. Irschik, Y., Nader, M. (2008) A Corollary to Mohr's Analogy for Optimal Placement of Piezoelectric Actuator Patches in Beams. *Proc. of 4th European Conf. on Structural Control,* Saint-Petersburg, Sept. 8-12, 2008, **V.1**, pp.351-357.
19. Duffy, K.P., and oth. Passively Shunted Piezoelectric Damping of Centrifugally-Loaded Plates. *Proc. on the 50th AIAA/ASME/ASCE/AHS/ASC Conf.* Palm Springs, Ca. p.10
20. Agnes, G.S. (1995) Development of a Modal Model for Simultaneous Active and Passive Piezoelectric Vibration Suppression. *J. of Intelligent Material Systems and Structures*. V.6, pp.482-487
21. Fleming, A.J., Berhens, S., Moheimani, S.O.R. (2002) Optimization and implementation of piezoelectric shunt damping systems. *IEEE/ASME Trans. on Mechatronics*, **V.7**, pp. 87-94.
22. Anisetti, A., Shiryayaev, O.V., and Slater, J.C. (2008) Non-linear Shunting of Piezo Actuators for Vibration Suppression. *Proc. on the 49th AIAA/ASME/ ASCE/AHS/ASC Conf.* Schaumburg, IL. p.6
23. Lesieutre, G.A., Ottman, G.K., Hofmann, H.F. (2004) Damping as a result of piezoelectric energy harvesting. *J. of Sound and Vibration*. **V.269**, pp.991–1001
24. Minazara, E., Vasic, D., Costa, F., and Poulin, G. (2006) Piezoelectric diaphragm for vibration energy harvesting. *Ultrasonics*. **V.44**, pp.699–703
25. Tsai, M. and Wang, K. (1999) On the Structural Damping Characteristics of Active Piezoelectric Actuators with Passive Shunt. *J. of Sound and Vibration*. V.221(1), pp.1–22
26. Agneni, A., Mastroddi, F., and Polli G.M. (2003) Shunted piezoelectric patches in elastic and aeroelastic vibrations. *Computers & Structures*, **V.81**, pp.91–105
27. Moheimani, S.O.R. (2003) A survey of recent innovations in vibration damping and control using shunted piezoelectric transducers. *IEEE Trans. on Control Systems Technology*, **V.11**, pp. 482-494
28. Dosch, J.J., Inman, D.J., and Garcia, E. (1992) A Self-Sensing Piezoelectric Actuator for Collocated Control. *J. of Intelligent Material Systems and Structures*.V. 3; pp.166-185
29. Glaz, B., Friedmann P.P., and L.Liu (2008) Vibration Reduction and Performance Enhancement of Helicopter Rotors Using an Active/Passive Approach. *Proc. of 49th AIAA/ASME/ASCE/AHS/ASC Structures, Structural Dynamics, and Materials Conf., 7 – 10 April 2008, Shaumburg, Il*, p. 18
30. Chandrasekaran, S., Lindner, D.K. (2000) Power Flow through Controlled Piezoelectric Actuators. *J. of Intelligent Material Systems and Structures.* **V.11**, pp.469-481
31. Clark, W.W. (2000) Vibration Control with State-Switched Piezoelectric Materials. *J. of Intelligent Material Systems and Structures*. V.11, pp.263-271
32. Kauffman, J.L., Lesieutre, G.A. (2007) A Low-Order Model for the Design of Energy Harvesting Piezoelectric Devices. *Proc. on the 48th AIAA/ASME /ASCE/AHS/ASC Conf.* Honolulu, Hawaii. p.12
33. Liang, C., Sun, F.P. and Rogers, C.A. (1997) Coupled Electro-Mechanical Analysis of Adaptive Material Systems-Determination of the Actuator Power Consumption and System Energy Transfer. *J. of Intelligent Material Systems and Structures*. **V.8**, pp.335-343
34. Min, J.B. and oth. (2008) A Resonant Damping Study Using Piezoelectric Materials. *Proc. on the 49th AIAA/ASME/ASCE/AHS/ASC Conf.* Schaumburg, IL. p.10
35. Renno, J.M., Daqaq, M.F., and Inman, D.J. (2009) On the optimal energy harvesting from a vibration source. *J. of Sound and Vibration*. **V.320**, pp.386-405
36. Halevi, Y., Peled, I. (2009) Absolute Vibration Suppression (AVS) Control - Modeling, Implementation and Robustness. *Proc. Int. Conf. on Struct. Eng. Dynamics.* Ericeira, Portugal, June 22-24. p.8
37. Elliot, S.J. Global Vibration Control Trough Local Feedback. In *Adaptive Structures. Engineering Applications*. Eds. D.Wagg and oth., J. Wiley & Sons. pp.59-85
38. Alhazza, K.A., Majeed, M.A. (2008) Free Vibrations Stability Analysis and Control of a Cantilever Beam with Multiple Time Delay State Feedback. *Proc. on the 49th AIAA/ASME /ASCE/AHS/ASC Conf.* Schaumburg, IL. p.10
39. Baillargeon, B.P. Vel, S.S. (2005) Active Vibration Suppression of Sandwich Beams using Piezoelectric Shear Actuators: Experiments and Numerical Simulations. *J. of Intelligent Material Systems and Structures.* **V.16**, pp.517-530
40. Jin-Chein Lin, Nien, M.H. (2005) Adaptive control of a composite cantilever beam with piezoelectric damping-modal actuators/sensors. *Comp. Struct.* **V.70**, pp.170–176
41. Ulker, F.D., Nalbantoglu, V., Yong Chen, and Zimcik, D. (2009) Active Vibration Control of a Smart Fin. *Proc. on the 50th AIAA/ASME/ASCE/AHS/ASC Conf.* Palm Springs, Ca. p.10